

Focal conic flowers, dislocation rings, and undulation textures in smectic liquid crystal Janus droplets: Supplementary Information

Wei-Shao Wei,^{a,b} Joonwoo Jeong,^c Peter J. Collings,^{a,d} and A. G. Yodh^{a,b}

^a Department of Physics and Astronomy, University of Pennsylvania, Philadelphia, PA, USA

^b Laboratory for Research on the Structure of Matter (LRSM), University of Pennsylvania, Philadelphia, PA, USA

^c Department of Physics, Ulsan National Institute of Science and Technology (UNIST), Ulsan, Republic of Korea

^d Department of Physics and Astronomy, Swarthmore College, Swarthmore, PA, USA

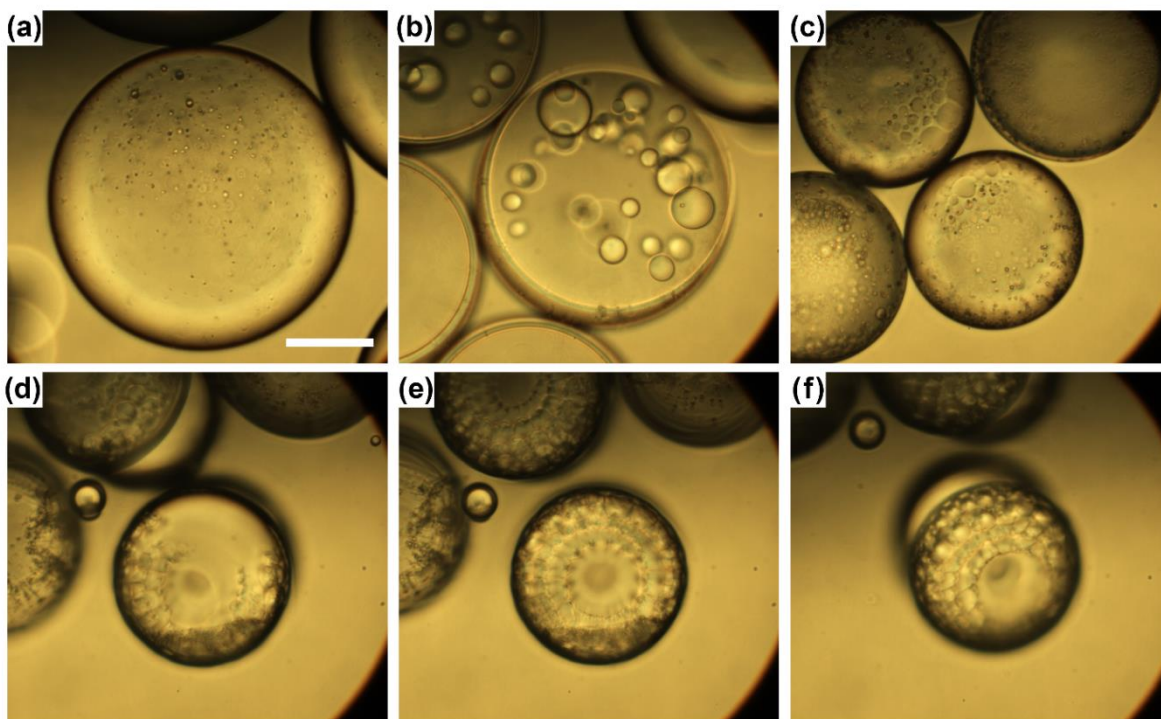


Fig. S1 Bright-field snapshots of the vigorous hydrodynamic flow observed during the first formation of Janus droplets. **(a)** The spherical droplet (containing fully miscible homogeneous mixtures of 8CB, PDMS, and hexane) suspended in a 0.1 wt% SDS water solution. **(b-c)** While the hexane evaporates from the droplet, or being more specific, during the process of solvent-induced phase separation, a turbulent-like vigorous mixing within drop is observed. **(d-f)** With the complete evaporation of hexane, the droplet then transforms from the initial homogeneous mixture to the targeted phase-separated Janus droplet, immediately followed by the formation of FCD textures within the LC compartment (pointing out of paper). The vigorous hydrodynamic flows are believed to randomize the system transiently, preventing the SmA LC from reaching its equilibrium configuration as stated in the main text. All images were captured at room temperature (~ 25 °C). Scale bar: 50 μm . Interested readers should also consult ESI Supplementary Video 1†.

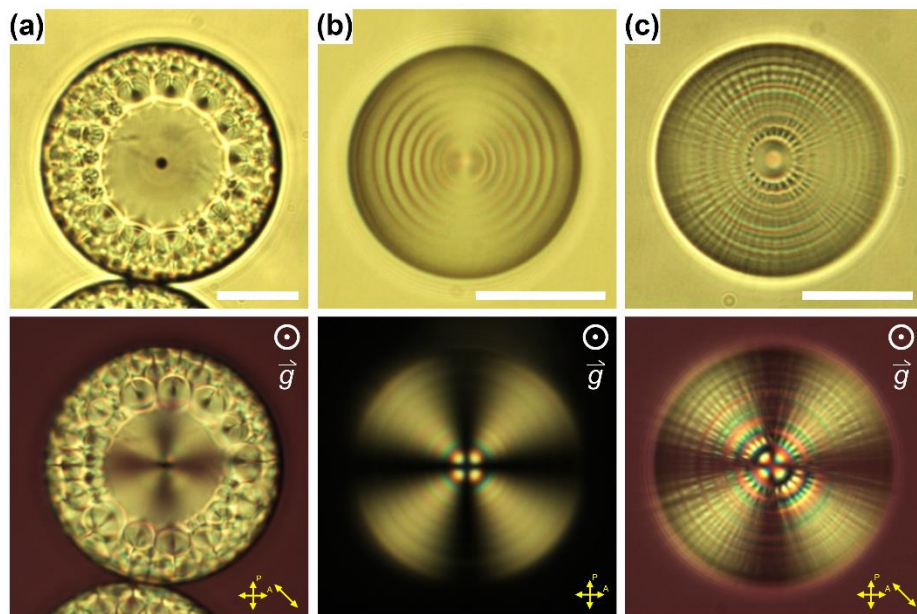


Fig. S2 FCD, dislocation, and undulation plus dislocation textures within Janus droplets. The bottom-view bright-field (top row) and POM (bottom row) images here show **(a)** FCD flower-like textures, **(b)** dislocation ring textures, and **(c)** textures with both undulations and dislocation rings for SmA LC confined in the bowl-shaped cavities of Janus droplets, after the initial droplet formation. Note, bottom panel of (b) was taken between cross-polarizers; bottom panels of (a) and (c) were taken between cross-polarizers and with a full-wave retardation plate. The vector \vec{g} in the figures denotes the direction of the gravitational acceleration. Scale bar: 20 μm . Interested readers should also consult Fig. 3 of the main text for more information.

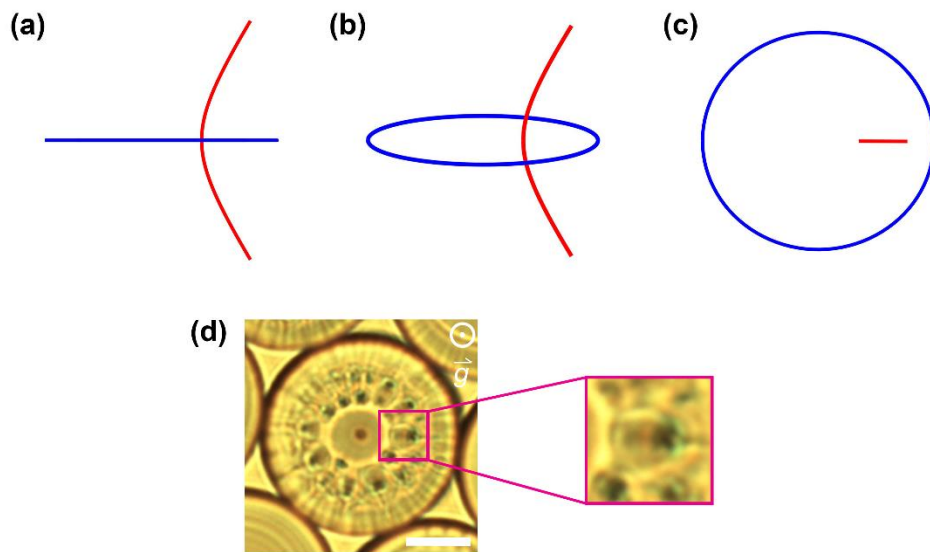


Fig. S3 Ellipse and hyperbola disclinations within a FCD. **(a-c)** Schematics of the conjugate ellipse (blue) and hyperbola (red) disclination (defect) curves within an individual FCD. (a) Side-, (b) tilt-, and (c) top-view of these two 3D-spanning conic sections are illustrated. **(d)** Bottom-view bright-field image of a Janus droplet with confined FCD flower-like texture (see also Fig. 3(b) in the main text). The inset (magnified image) highlights a single FCD, which corresponds to the sketch shown in (c). Scar bar: 10 μm .

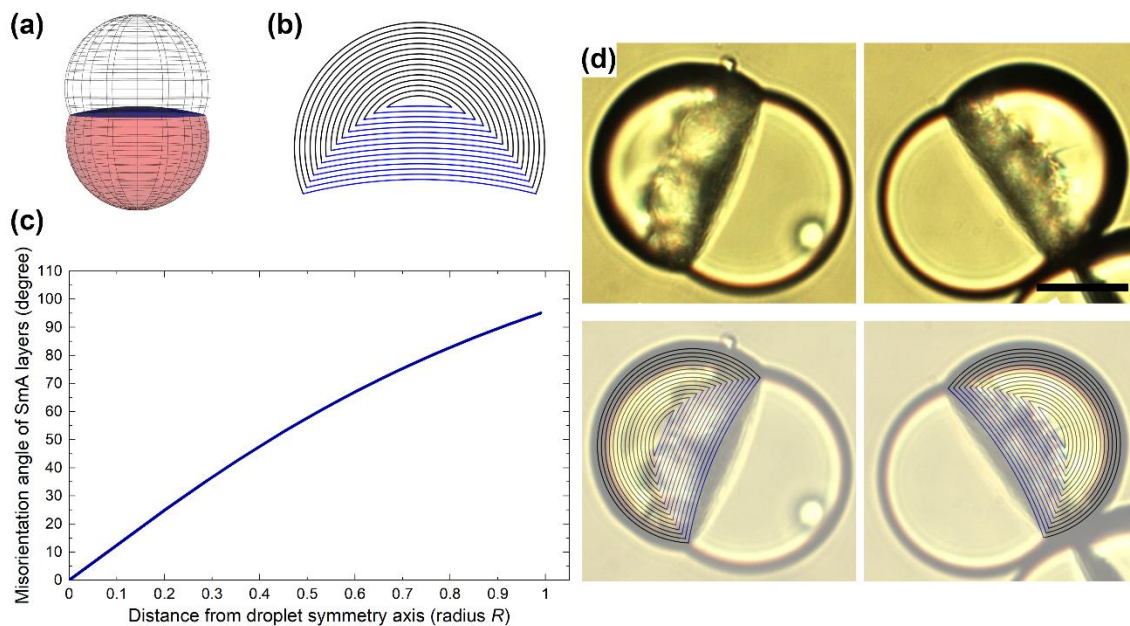


Fig. S4 Grain boundary misorientation angle and defect location within the bowl-shaped LC cavity of the Janus droplet. **(a)** Schematic 3D reconstruction of the Janus droplet (with 8CB as top compartment). The 8CB-PDMS, 8CB-water, and PDMS-water interfaces are color-coded as blue, black (the black frame on the transparent surface), and red, respectively. **(b)** Within the bowl-shaped LC compartment cavity, we propose a simplified model of the smectic layers, which exhibits a structure similar to that of the “deformed spherical onion” configuration. Here, two sets of SmA layers are sketched (shown in cross-section). The black curves represent layers that are parallel to and equidistant from the 8CB-water interface; the blue curves represent layers that are parallel to and equidistant from the 8CB-PDMS interface. A misorientation arises when these two sets of smectic layers meet but have different orientations. The resulting grain boundary, *i.e.*, the interface where misorientation of smectic layers occurs, hints at the locations of defects. **(c)** From the smectic layer schematic, the grain boundary misorientation angle (*i.e.*, the angle between the two sets of smectic layers, one set (shown in black) near the 8CB-water interface and the other set (shown in blue) near the 8CB-PDMS interface) can be calculated. It is plotted as a function of radial distance from the droplet central symmetry axis. **(d)** Smectic layers and grain boundary schematic (shown in (b)) overlaid on two side-view bright-field images of Janus droplets with FCDs in their LC compartment. (Top panel: bright-field images. Bottom panel: overlays.) The good agreement between proposed model and experimental observation suggests that the defects (*e.g.*, FCDs) are located on grain boundaries. Scale bar: 20 μm .

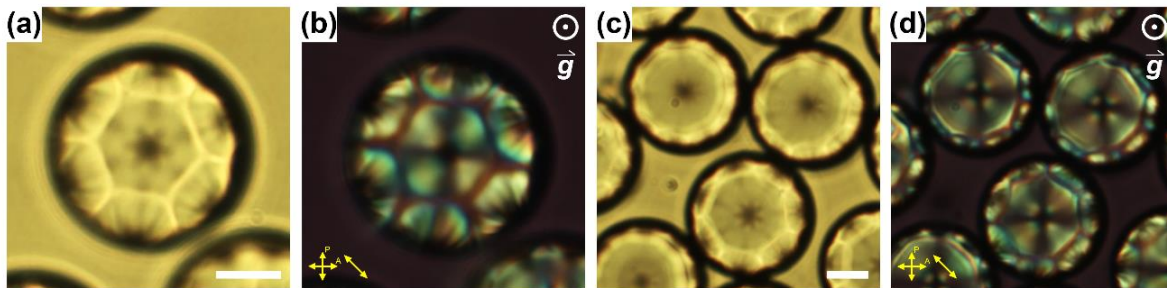


Fig. S5 Focal conic textures within Janus droplets at high SDS concentration. **(a-b)** The bottom-view (a) bright-field and (b) POM (coupled with a full-wave retardation plate) image of SmA Janus droplets in a 0.5 wt% SDS water solution, which is above the critical micelle concentration CMC. Note, the FCDs within each droplet seem to extend to the drop surface, showing configurations different from the low SDS concentration case (consult Fig. 3(a) in the main text). **(c-d)** Similar FCD textures observed in another sample under the same experimental conditions. Scale bar: 10 μm . The vector \vec{g} in the figures denotes the direction of the gravitational acceleration. Interested readers should also consult ESI Supplementary Video 2† for the focal conic texture formation process upon phase transition.

Supplementary Video 1 | The vigorous hydrodynamic flow observed during the first formation of Janus droplets. The size of a suspended spherical droplet (which contains a homogeneous mixture of 8CB, PDMS, and hexane) shrinks as the hexane evaporates through the background continuous phase (*i.e.*, a 0.1 wt% SDS water solution). During this process, vigorous hydrodynamic (mixing) flows can be observed. The complete evaporation of hexane then causes separation of the immiscible 8CB and PDMS, leading to the target geometry of a Janus droplet. Meanwhile, FCD textures form within the LC (8CB) compartment. Images were taken at room temperature (~25 °C) and between crossed-polarizers with a full-wave retardation plate. The purple color indicates the isotropic phase; the birefringence can only be observed upon formation of liquid crystalline order (*i.e.*, upon the complete evaporation of hexane). The time stamp 00:00 denotes minute: second. The video is sped up by 20x.

Supplementary Video 2 | Formation of focal conic textures within Janus droplets suspended in concentrated SDS solution upon phase transition. Multiple Janus droplets are shown in the field-of-view, suspended in a 0.5 wt% SDS (above CMC) water solution with their LC compartments roughly pointing out of the screen. Images were taken between crossed-polarizers with a full-wave retardation plate, permitting visualization of director fields (orange indicates northwest-southeast alignment; cyan indicates northeast-southwest alignment). At high temperature (~36 °C, 00:00:00), the 8CB in the LC compartments is in its nematic phase and exhibits a radial configuration. As the system temperature decreases gradually toward room temperature (~25 °C), the 8CB undergoes a phase transition from nematic to SmA, immediately followed by the formation of bud-like focal conic textures (00:46:00). The time stamp 00:00:00 denotes minute: second: 1/60 second. The video is sped up by 2x.

Supplementary Video 3 | SmA texture transition from the FCD flowers to the dislocation rings during thermal annealing. A single Janus droplet suspended in a 0.1 wt% SDS water solution is shown in the field-of-view, with its LC compartment pointing out of the screen. At room temperature (~25 °C, 00:00:00), the 8CB is in the SmA phase, exhibiting FCD flower textures. The FCD textures “melt” as the system temperature increases and the 8CB undergoes a phase transition through the nematic phase (roughly above 33 °C, 00:20:00) to the isotropic phase (roughly above 40 °C, 00:42:00), wherein the birefringence disappears. Then, as the system temperature is decreased again, the 8CB shows the nematic phase (00:50:00) first and eventually exhibits the SmA phase (1:36:00). Formation of the dislocation ring textures, which suffuse the entire cavity in a sequential manner, in the SmA phase can then be observed. Note, the FCD textures do not reoccur after annealing. Images were taken between crossed-polarizers with a full-wave retardation plate. The time stamp 00:00:00 denotes minute: second: 1/60 second. The video is sped up by 3x.

Supplementary Video 4 | SmA dislocation ring textures further evolve into a state of undulations plus dislocation rings after relaxation. An annealed Janus droplet, which is already in its SmA phase and exhibits dislocation ring textures, is shown at the center of the field-of-view (~25 °C, 00:00). The droplet has its LC compartment pointing out of the screen. Starting from 00:14, smectic undulations appear on top of the existing dislocation rings, further relaxing the SmA Janus droplet into its equilibrium states. Also, our observations suggest that the textures always form and suffuse the entire cavity in a sequential manner. Note, this video was captured a few minutes after the annealing protocol (at approximately constant system temperature), while the typical relaxation process is much slower and could take several hours or up to days. Images were taken between crossed-polarizers with a full-wave retardation plate. The time stamp 00:00 denotes minute: second. The video is sped up by 10x.